

## **Supplemental Materials**

### **Protein splicing of a recombinase intein induced by single-stranded DNA and DNA damage**

Christopher W. Lennon, Matthew Stanger, and Marlene Belfort\*

\*Correspondence to Marlene Belfort ([mbelfort@albany.edu](mailto:mbelfort@albany.edu)).

#### **This PDF includes:**

**Supplemental Figures 1-6**

**Supplemental Figure Legends**

**Supplemental Tables 1-3**

**Supplemental Reference**

## Supplemental Figure Legends

**Supplemental Figure 1:** Characteristics of ssDNA-stimulated RadA splicing. *(A)* ATP does not accelerate  $\Delta$ N-RadA splicing in the presence or absence of ssDNA. Reaction mixtures were incubated at 63°C for 10 min, separated by SDS-PAGE, and stained with Coomassie. See Figure 1A for band assignment. Below, bar graph quantitation of the gel in panel *A*. *(B)* Full-length RadA splices in response to ssDNA. Samples were treated at 63°C for the indicated times and processed as in panel *A*. Below, bar graph quantitation of the gel in panel *B*. *(C)* Splicing is not stimulated by dsDNA. M13mp18 ssDNA stimulates splicing, while M13mp18 dsDNA (replicative form 1), which has the same sequence, does not. Below, bar graph quantitation of the gel in panel *C*. *(D)* Increased secondary structure of ssDNA decreases RadA splicing stimulation. Increasing MgCl<sub>2</sub> concentration decreases the effect of ssDNA but not of splicing in the absence of ssDNA. Below, bar graph quantitation of the gel in panel *D*. Data in all panels are representative of at least 3 experiments.

**Supplemental Figure 2:** RadA Binding to ssDNA. *(A)* RadA-R503A is defective in ssDNA binding.  $\Delta$ N-RadA and the  $\Delta$ N-RadA-R503A mutant bind to ssDNA, with  $\Delta$ N-RadA-R503A showing ~3-fold lower affinity. Both  $\Delta$ N-RadA  $\Delta$ N-RadA-R503A were spliced prior to incubation. The concentration of ssDNA is 5  $\mu$ M binding sites (3 bases per RadA binding site; Seitz et al. 1998) and concentrations of RadA are listed above each lane. *(B)* Free RadA intein does not bind to ssDNA. The concentration of ssDNA is 16.7  $\mu$ M binding sites and concentrations of the free intein are listed above each lane. A higher concentration of ssDNA was used in panel *B* compared panel *A*

and Fig. 1a to promote interaction. Samples in panels A and B were incubated at 63°C for 60 min and separated on a 1% agarose gel. (C) Apparent  $K_d$  determination. The fraction of ssDNA bound at different RadA protein concentrations from 3 independent binding experiments for  $\Delta N$ -RadA,  $\Delta N$ -RadA-AA (trapped precursor; see Fig. 1B) and  $\Delta N$ -RadA-R503A. See Materials and Methods for details on curve fitting.

**Supplemental Figure 3:** RadA intein in foreign exteins is unaffected by ssDNA. (A) RadA splicing in the MIG construct, where maltose binding protein is the N-extein and green fluorescent protein the C-extein. Following expression from pMIG-RadAi at 30°C for 1 h and cell lysis, lysate was incubated at 23°C with or without M13mp18 ssDNA for indicated times, separated by SDS-PAGE, and visualized using in-gel fluorescence. P, precursor conformers; LE, ligated exteins. (B) Quantitation of panel A based on fluorescence. Dashed line is without ssDNA, solid line is with ssDNA.

**Supplemental Figure 4:** Concentration and temperature-dependent RadA splicing. (A) Splicing stimulation by ssDNA is greater at reduced protein concentration. Reactions were incubated at 63°C for 10 min. Below, quantitation of the gel in panel A. (B) ssDNA accelerates  $\Delta N$ -RadA splicing at 37°C. Reactions were incubated at 37°C for indicated times, and processed as above. Below, quantitation of the gel in panel B. Data in all panels are representative of at least 3 experiments.

**Supplemental Figure 5:** RadA splicing in the absence of DNA damage and following UV treatment in SOS<sup>-</sup> and SOS<sup>+</sup> strains. (A) RadA splicing in absence of DNA damage in SOS<sup>-</sup> and SOS<sup>+</sup> strains. RadA was expressed in *E. coli* at 37°C in *lexA*<sup>+</sup> and *lexA3* in the absence of external stress (Supplemental table 3 for genotypes). Precursor (P) and ligated exteins (LE) were isolated by his-tag mediated pull-down, separated by SDS-PAGE, stained with Coomassie, and the amounts of P and LE were determined by densitometry. Precursor resolves as 2 bands when expressed at 37°C as previously described (Topilina et al. 2015b). (B) Quantitation of splicing in panel A. (C) Splicing in SOS<sup>+</sup> strains is higher than in SOS<sup>-</sup> after UV treatment. Expression of RadA in *recA*<sup>+</sup>/*recA*<sup>-</sup> and *lexA*<sup>+</sup>/*lexA3* strain pairs was measured 2 h after UV treatment. Samples were isolated and analyzed as in panel A.

**Supplemental Figure 6:** DNA-binding residue required for maximal ssDNA splicing enhancement. (A) *Pho* RadA residue R503 is highly conserved in nature. The alignment was generated using Clustal Omega. (B) RadA precursor model showing pertinent features. Pymol was employed to generate the image using the model of precursor (Topilina et al. 2015b). N-extein (residues 1-115 omitted), blue; Intein, red; C-extein, green; L1 and L2, yellow; Intein C1 (C153), rose spacefill; C-extein T+1 (T325), lime green spacefill; R503, dark green spacefill (C).  $\Delta$ N-RadA-R503A splicing stimulation by ssDNA is reduced. Reactions were incubated at 63°C and analyzed as in Figure 2. (D) Kinetics of  $\Delta$ N-RadA-R503A splicing stimulation. Plots are in the presence (filled circles) and absence (open circles) of ssDNA. Error was calculated as the standard deviation from 3 independent experiments. When error bars are

not shown, error is less than the size of the symbol. Also displayed for reference are the curves of  $\Delta N$ -RadA splicing with and without ssDNA from Fig. 2B to 180 min (gray).

### Supplemental Table 1. List of oligonucleotides used in this study

Oligo ID	Sequence (5' → 3')	Application
IDT3557	CCCGGATCCGATTGGAAGGATCTCAACTGGAAGCAAAAGTTTAG	pΔN-RadAi and pΔN-RadAi-AA cloning
IDT3558	CCCGGATCCGAAAGCATTGGAAGGATCTCAACTGGAAGC	pΔN-RadAi and pΔN-RadAi-AA cloning
IDT3674	GAAGGGTAAGGGAGGAAAGCGGTAGCTAGGTTAATAGAT	pΔN-RadAi R503A mutagenesis
IDT3675	ATCTATTAACCTAGCTACCGCCTTTCCTCCCTTACCCTTC	pΔN-RadAi R503A mutagenesis
IDT4172	CCTGCCTTGTGGCAGCTTCAAGAATTCGGTAGTGGGAAGTGCTTTGCTAGG	pXI-INT-RadA cloning
IDT4173	GTAAAACGACGGCCAGTGCCAAGCTTTTATTAAGCATGGAGAACAAGTCCATTGGGAGC	pXI-INT-RadA cloning

### Supplemental Table 2. List of plasmids used in this study

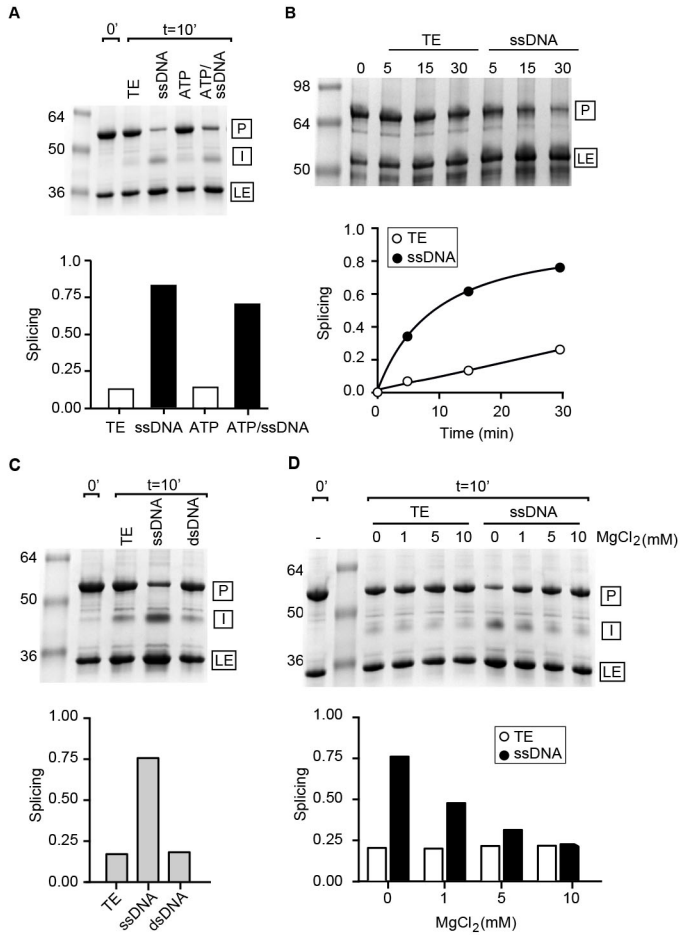
Plasmid	Comments	Source
pΔN-RadAi	For expression of intein containing <i>Pho</i> RadA lacking residues 1-115 with an amino-terminal his-tag lacking cloned into <i>Bam</i> HI/ <i>Xho</i> I sites of pET45b(+)	Present study
pΔN-RadAi-AA	C153A, N324A splicing inactive mutant of pΔN-RadAi	Present study
pΔN-RadAi-R503A	R503A mutant of pΔN-RadAi	Present study
pXI-INT-RadA	<i>Pho</i> RadA Intein with chitin binding domain; no RadA extein sequence	Present study
pMIG-RadAi	<i>Pho</i> RadA intein with short extein sequences cloned between MBP and GFP	Topilina et al. 2015b
pFL-RadAi	For expression of full-length intein containing <i>Pho</i> RadA precursor with an amino-terminal his-tag	Topilina et al. 2015b
pFL-RadAi-AA	C153A, N324A splicing inactive mutant of pFL-RadAi-AA	Topilina et al. 2015b

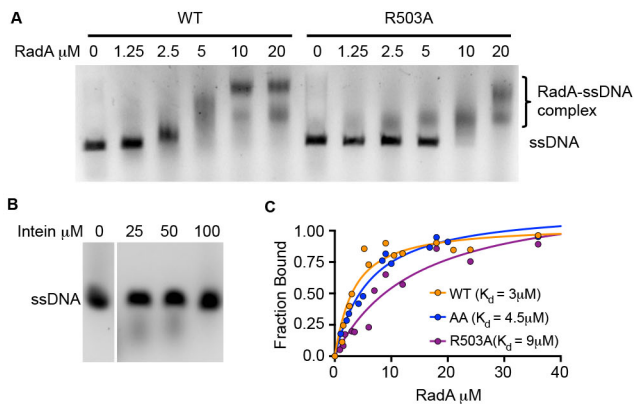
**Supplemental Table 3. List of *E. coli* strains used in this study**

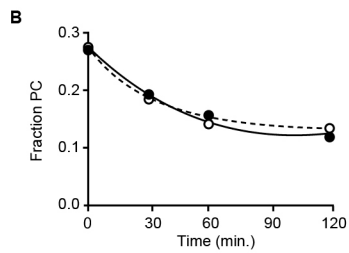
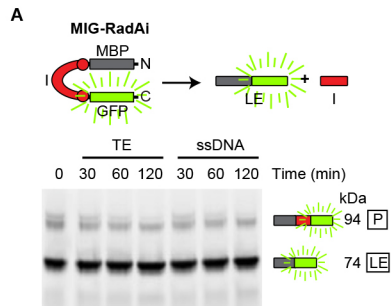
Strain	Genotype	Source
AB1157(DE3)	<i>F'</i> <i>thr1 leuB6 Δ(gpt-proA)2 hisG4 argE3 thi-1 ara-14 lacY1 galK2 xyl-5 mtl-1 rpsL31 tsx-33 supE44 (rac) λ</i> (DE3)	Smith et al. 2005
AB1157 <i>lexA3</i>	<i>F'</i> <i>thr1 leuB6 Δ(gpt-proA)2 hisG4 argE3 thi-1 ara-14 lacY1 galK2 xyl-5 mtl-1 rpsL31 tsx-33 supE44 (rac) lexA3zja::Tn10</i> (Tet <sup>r</sup> )	Richard P. Cunningham, pers. comm.
AB1157 <i>lexA3</i> (DE3)	<i>F'</i> <i>thr1 leuB6 Δ(gpt-proA)2 hisG4 argE3 thi-1 ara-14 lacY1 galK2 xyl-5 mtl-1 rpsL31 tsx-33 supE44 (rac) λ</i> (DE3) <i>lexA3zja::Tn10</i> (Tet <sup>r</sup> )	Present study
ArcticExpress(DE3)	<i>F</i> <sup>-</sup> <i>ompT hsdS<sub>B</sub>(r<sub>B</sub><sup>-</sup> m<sub>B</sub><sup>-</sup>) dcm gal λ</i> (DE3) <i>endA Hte [cpn10 cpn60 Gent<sup>r</sup>]</i> (Tet <sup>r</sup> )	Agilent
BL21(DE3)	<i>F</i> <sup>-</sup> <i>ompT hsdS<sub>B</sub>(r<sub>B</sub><sup>-</sup> m<sub>B</sub><sup>-</sup>) gal dcm</i> (DE3)	Novagen
BLR(DE3)	<i>F</i> <sup>-</sup> <i>ompT hsdS<sub>B</sub>(r<sub>B</sub><sup>-</sup> m<sub>B</sub><sup>-</sup>) gal dcm</i> (DE3) <i>Δ(srl-recA)306::Tn10</i> (Tet <sup>r</sup> )	Novagen
JM109	<i>F'</i> <i>traD36 proA<sup>+</sup>B<sup>+</sup> lacI<sup>q</sup> Δ(lacZ)M15/ Δ(lac-proAB) glnV44 e14<sup>-</sup> gyrA96 recA1 relA1 endA1 thi hsdR17</i>	New England Biolabs

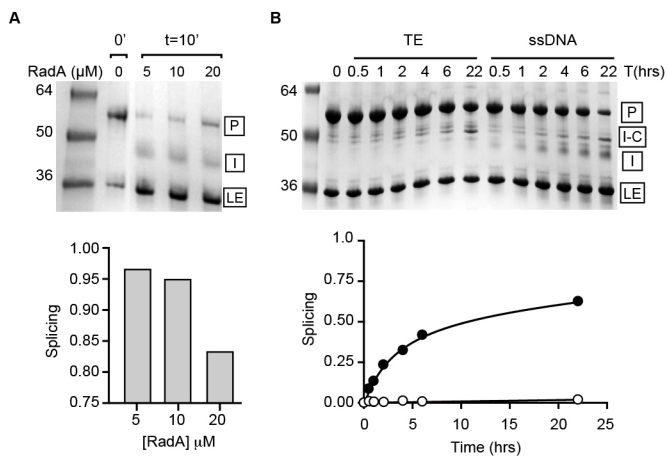
**Supplemental Reference**

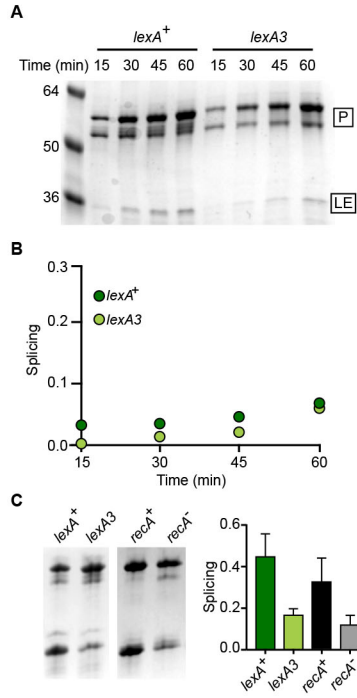
Smith D, Zhong J, Matsuura M, Lambowitz AM, Belfort M. 2005. Recruitment of host functions suggests a repair pathway for late steps in group II intron retrohoming. *Genes Dev* **19**: 2477-2847.











**A**

<i>P. horikoshii</i>	RadA	494-YLRKGGKGGK	RLIDAPHLPEG-513
<i>P. furiosus</i>	RadA	314-YLRKGGKGGK	RIARLIDAPHL-333
<i>M. voltae</i>	RadA	287-FVRKGGKGDK	RVAKLYDSPHL-306
<i>S. cerevisiae</i>	Rad51	359-GFKKGGKGCQ	RLCKVVDSPL-378
<i>H. sapien</i>	Rad51	301-YLRKGRGET	RIKCIYDSPCL-320

